

A Novel Method for Medical Implant In-Body Localization

Mohammad Pourhomayoun, *Student Member, IEEE*, Mark Fowler, *Senior Member, IEEE* and Zhanpeng Jin, *Member, IEEE*

Abstract—Wireless communication medical implants are gaining an important role in healthcare systems by controlling and transmitting the vital information of the patients. Recently, Wireless Capsule Endoscopy (WCE) has become a popular method to visualize and diagnose the human gastrointestinal (GI) tract. Estimating the exact location of the capsule when each image is taken is a very critical issue in capsule endoscopy. Most of the common capsule localization methods are based on estimating one or more location-dependent signal parameters like TOA or RSS. However, some unique challenges exist for in-body localization due to the complex nature within the human body, such as multipath caused by the boundaries of the organs, shadowing effect, and the fact that the signal propagation velocity and path loss parameters are not constant inside the entire human body. Furthermore, the use of high-band or high power signals for implant localization is restricted by defined standards (i.e., MICS). In this paper, we propose a novel one-stage localization method based on spatial sparsity in 3D space. In this method, we directly estimate the location of the capsule (as the emitter) without going through the intermediate stage of TOA or signal strength estimation. We evaluate the performance of the proposed method using Monte Carlo simulation with an RF signal following the allowable power and bandwidth range according to the standards. The results show that the proposed method is very effective and accurate even in massive multipath and shadowing conditions.

Index Terms— Medical Implant, Capsule Endoscopy, Time of Arrival (TOA), Received Signal Strength (RSS), Sparsity.

I. INTRODUCTION

Wireless communication devices for medical applications have attracted lots of attention recently. Wearable and implantable medical devices such as body sensors, smart pills, pacemakers and so on are gaining important roles in health care systems by controlling and transmitting the vital information of the patients. Recent developments in semiconductor technology also enables designing smaller and cheaper medical wireless devices that are more convenient to be worn or implanted inside a human body for special medical interventions.

Recently, Wireless Capsule Endoscopy (WCE) has become a preferred method to visualize and diagnose the human gastrointestinal (GI) tract [1]. Capsule Endoscopy has advantages for both patient and physician since it is non-invasive, more precise and even portable [1][2]. Contrary to traditional methods such as Gastroscopy and Colonoscopy that can only reach the first or last several feet of the GI tract, the capsule endoscopy allows the visualization of the entire gastrointestinal tract [3].

Since the physicians need to know the exact location of the capsule when each image is taken in the process of endoscopy, precise capsule localization is imperative in capsule endoscopy [1][2] and has been widely investigated recently [1]-[10]. Among all different methods that have been suggested for capsule localization, RF signal based methods have the advantage of application-non-specific property and relatively low-cost hardware implementation [1][3].

The standard, Medical Implant Communication Services (MICS), allows two-way communication with medical implants in frequency band 401-406 MHz with the maximum bandwidth of 300 KHz and maximum transmitted power of 25 μ w [2]. It is therefore desirable to have localization methods that are effective under these constraints.

The classic approaches to RF signal based localization methods are to first estimate one or more location-dependent signal parameters such as time-of-arrival (TOA), angle-of-arrival (AOA) or received-signal-strength (RSS). In this step, the emitter (implant) propagates an RF signal and sensors (on the body surface) receive the transmitted signal (as shown in figure 1) and try to estimate the location-dependent parameter. Then in a second step, the collection of the estimated parameters is used to determine an estimate of the emitter's location. The methods based on time-of-arrival (TOA) are usually more accurate compared to the RSS or AOA based methods. In [2], the authors make a comparison between RSS based methods and traditional TOA based methods (like in [4]) for the purpose of capsule localization. The results show that the TOA based methods achieve more accurate results compared to RSS. However, the accuracy of traditional TOA based methods usually suffers from multipath conditions caused by signal reflections at the boundaries of body organs [4].

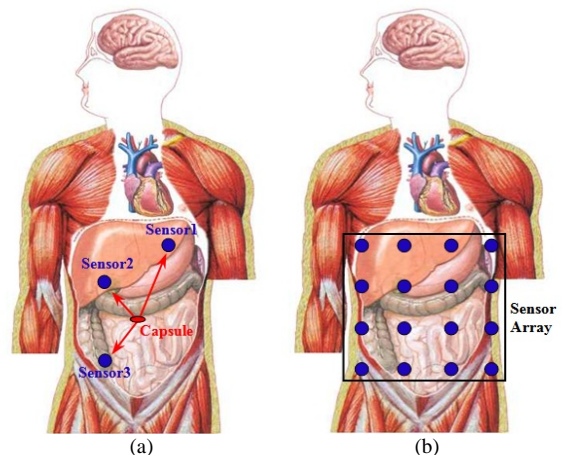


Figure (1): (a) Capsule and sensors configuration for three sensors. (b) Sensor array mounted on body surface or mounted inside a wearable jacket.

Since the human body includes various organs with different types of tissues, the electrical characteristics of the entire body show vast heterogeneity and anisotropy, such as the conductivity, power absorption, path loss, and relative permittivity. For example, the relative permittivity value varies for different tissues and since the signal propagation velocity is expressed as a function of the relative permittivity, the propagation velocity and consequently the time-of-arrival highly depends on the tissue where the signal passes through from implant to the sensor [4]. The power absorption parameters and path loss exponent also varies by thickness of the tissue [11] and it necessitates to have some prior information about the location of the implant in traditional RSS based methods.

In [4], the authors suggested an iterative method based on TOA estimation. In this method, the tissue configuration of the human body is acquired beforehand from MRI or CT system. Having this model, the *average* relative permittivity and the propagation velocity are computed. The time-of-arrival (TOA) for each sensor is also estimated using correlation methods. Then, the estimated TOAs and *average* relative permittivity are used to estimate the approximate implant location by least square methods. In the next step, the approximate location is used to find a more accurate permittivity, propagation velocity and finally the more accurate location estimation. However, like other traditional TOA based methods, the TOA estimation stage suffers from multipath conditions. In this method, the authors use ultra wideband (UWB) signal to achieve higher resolution in TOA estimation. However, UWB signals are not compliant with the Medical Implant Communication Services (MICS) standard.

In this paper, we develop a novel tissue-adaptive one-stage method based on both time-of-arrival and path loss. We take advantage of spatial sparsity of the emitter in the 3D space to estimate the emitter location. In this method, we use convex optimization theory to estimate the location of the emitter directly without going through the intermediate stage of TOA or path loss estimation. Since we don't need to estimate the time-of-arrival for each one of the sensors by its own in a separate stage and we also exploit the spatial sparsity to estimate the emitter location directly, this method is very robust to multipath conditions compared to traditional TOA based methods.

It is manifest that in emitter localization problems, the number of emitters is much smaller than the number of all grid points in a fine grid on the x-y plane in a two-dimensional case or x-y-z space in a three-dimensional scenario. Thus, by assigning a positive number to each one of the grid points containing an emitter and assigning zeros to the rest of the grid points, we will have a very sparse grid matrix that can be reformed as a *sparse vector*. In this context, a *sparse vector* is a vector containing only a small number of non-zero elements [12]. Since each element of this grid vector corresponds to one grid point in the x-y-z space, we can estimate the location of emitters by extracting the position of non-zero elements of the sparsest vector that

satisfies the delay relationship between transmitted signals and received signals.

In principle, sparsity of the grid vector can be enforced by minimizing its ℓ_0 -norm which is defined as the number of non-zero elements in the vector. However, since the ℓ_0 -norm minimization is an NP-hard non-convex optimization problem, it is very common (e.g in compressive sensing problems) to approximate it with ℓ_1 -norm minimization, which is a convex optimization problem and also achieves the sparse solution very well [12]. Thus, after formulating the problem in terms of the sparse grid vector, we can estimate this vector by pushing sparsity using ℓ_1 -norm minimization on the grid vector, subject to the delay relationship between the signals transmitted from the grid point and the signals received by the sensors.

As mentioned above, contrary to classic methods, in this paper we directly estimate the location of the emitter without going through the intermediate stage of time-of-arrival or path loss estimation. We will see this method is very robust and very effectively deals with multipath, which is a serious problem in implant localization due to the reflections from organ boundaries.

We evaluate the performance of the proposed method by Monte Carlo computer simulations in massive multipath and shadow fading conditions. The simulation results show the accurate localization and high performance of this method even with low SNRs and with small number of sensors; this provides a significant advantage over traditional two-stage methods based on TOA or RSS.

II. PROBLEM FORMULATION

Suppose that an emitter transmits a signal and L sensors receive that signal. The complex baseband signal observed by the i^{th} sensor is

$$r_i(t) = \alpha_i s(t - \tau_i) + n_i(t) \quad (1)$$

where $s(t)$ is the transmitted signal, τ_i is the signal delay, α_i is the path attenuation, and $n_i(t)$ is a white, zero mean, complex Gaussian noise.

There are two big differences for localization inside the human body compared to localization in other environments. The first difference is the intense RF signal absorption by body tissues that causes a remarkable path loss. The second difference is the dependence of the signal propagation velocity on the tissue where the signal is passing through. In our model in (1), we exploit these characteristics as location-dependent parameters to achieve more accurate estimation rather than considering them as difficulties.

In equation (1), α_i represents the path loss in addition to a constant phase shift [13][14]. The path loss model in dB is given by [11],

$$PL(d) = PL(d_0) + 10\beta \log_{10}(d/d_0) + S, \quad d \geq d_0 \quad (2)$$

where $PL(d)$ is the path loss at distance d , $PL(d_0)$ is the path loss at the reference distance d_0 (i.e. 50 mm), β is the path loss exponent value and S is a zero mean Gaussian random variable (in dB) representing the shadowing effect, $S \sim N(0, \sigma_s^2)$ [1],[11]. Table I shows the path loss parameters for the implant to body surface model [11].

TABLE I. PATH LOSS PARAMETERS: IMPLANT TO BODY SURFACE MODEL

Implant to Body Surface	PL(d_0) (dB)	β	σ_s (dB)
Deep Tissue	47.14	4.26	7.85
Near Surface	49.81	4.22	6.81

In free space, we can easily assume that the signal propagation velocity is constant. However, as mentioned above, for localization inside the human body the propagation velocity is not constant. The signal propagation velocity in a homogeneous tissue is given by [4],

$$v(\omega) = \frac{c}{\sqrt{\epsilon_r(\omega)}} \quad (3)$$

where $v(\omega)$ is the propagation velocity at frequency ω , c is the velocity of light in the free space and $\epsilon_r(\omega)$ is the relative permittivity of a human body tissue at frequency ω [4]. As we see in (3), the relative permittivity is frequency dependent. However, the values and curves for relative permittivity are available for various frequencies and different tissues (such as muscle, fat, bone, stomach, intestine and so on) [4][15][16]. We can calculate the average relative permittivity and average velocity for the path which the signal is traveling as follows [4],

$$v_{avg} = \frac{c}{\sqrt{\epsilon_{avg}}} \quad (4)$$

$$\epsilon_{avg} = \sum_{i=1}^{N_l} \epsilon_i p_i,$$

where N_l is the number of different tissues on the path from the emitter to the sensor, ϵ_i is the relative permittivity of i^{th} tissue at desired frequency and p_i is the percentage of each tissue on the path. As in [4], we are able to calculate the v_{avg} for each path using the equation (4) having the tissue configuration of the human body acquired beforehand from MRI or CT system.

Assume that each sensor collects N_s signal samples at sampling frequency $F_s = 1/T_s$. Then we have

$$\mathbf{r}_l = \alpha_l \mathbf{D}_l \mathbf{s} + \mathbf{n}_l \quad (5)$$

where $\mathbf{r}_l \triangleq [r_l(t_1), r_l(t_2), \dots, r_l(t_{N_s})]^T$ is the vector containing N_s samples of the received signal by l^{th} sensor, $\mathbf{s} \triangleq [s(t_1), s(t_2), \dots, s(t_{N_s})]^T$ is N_s samples of the transmitted signal, \mathbf{n}_l is the noise vector and \mathbf{D}_l is the time sample shift operator by $k_l = (\tau_l / T_s)$ samples where $\tau_l = (d_l / v_{avg,l})$ is delay, d_l is the distance between emitter

and the l^{th} sensor and $v_{avg,l}$ is the average velocity on the path from emitter to the l^{th} sensor derived from (4). We can write $\mathbf{D}_l = \mathbf{D}^{k_l}$ where \mathbf{D} is an $N_s \times N_s$ permutation matrix defined as $[\mathbf{D}]_{ij} = 1$ if $i = j+1$, $[\mathbf{D}]_{0,N-1} = 1$ and $[\mathbf{D}]_{ij} = 0$ otherwise.

$$\mathbf{D} = \begin{bmatrix} 0 & & & 1 \\ 1 & 0 & & \\ & \ddots & \ddots & \\ 0 & & 1 & 0 \end{bmatrix}, \quad \mathbf{D}_l = \begin{bmatrix} 0 & & & 1 \\ 1 & 0 & & \\ & \ddots & \ddots & \\ 0 & & 1 & 0 \end{bmatrix}^{k_l}$$

To simplify the notations, we assume that we are interested in estimating the location of the target in the two-dimensional (x - y) plane. It is easy to expand the localization problem to the three-dimensional case.

Now, we assign a number $\zeta_{x,y}$ to each one of the grid points (x,y) . Assume that $\zeta_{x,y}$ is one for the grid points containing an emitter and zero for the rest of the grid points. Thus, the signal vector received by l^{th} sensor will be

$$\mathbf{r}_l = \sum_x \sum_y \zeta_{x,y} \alpha_{l,x,y} \mathbf{D}_{l,x,y} \mathbf{s} + \mathbf{n}_l, \quad (6)$$

where $\mathbf{D}_{l,x,y}$ is the time sample shift operator w.r.t sensor l assuming that the emitter is located in the grid point (x,y) and the summations are over all grid points in the desired (x,y) range. Note that $\mathbf{D}_{l,x,y}$ and $\alpha_{l,x,y}$ are known in (6) since the location of the sensor l and each grid point (x,y) is known and we are able to find the delay and the path loss from (2) and (4) for the distance from grid point (x,y) to the sensor l . The unknown term is $\zeta_{x,y}$ that represents which one of the grid point contains the emitter (i.e capsule). Now, if we reform all of the grid points in a column vector and rearrange the indices, we will have

$$\mathbf{r}_l = \sum_{n=1}^N \zeta_n \alpha_{l,n} \mathbf{D}_{l,n} \mathbf{s} + \mathbf{n}_l. \quad (7)$$

The only difference between two-dimensional and three-dimensional localization is that the vector ζ_n will be longer in three-dimension case since it is formed by more grid points.

Now, we define the matrix Λ_n as the delay operator w.r.t all L sensors, assuming that the received signal comes from the grid point n (there is an emitter at grid point n):

$$\Lambda_n \triangleq \begin{bmatrix} \alpha_{1,n} \mathbf{D}_{1,n} & \alpha_{2,n} \mathbf{D}_{2,n} & \cdots & \alpha_{L,n} \mathbf{D}_{L,n} \end{bmatrix}_{N_s \times LN_s}$$

Then, we can define $\theta_n, n \in \{1, 2, \dots, N\}$ as an $LN_s \times 1$ vector containing all signals received by all L sensors when the emitter is in grid point n as,

$$\boldsymbol{\theta}_n \triangleq \Lambda_n^T \times \mathbf{s}_n \quad (8)$$

where $(\cdot)^T$ is the matrix transpose.

Now, if we arrange all vectors $\boldsymbol{\theta}_n$ for $n:1\dots N$ as the columns of a matrix $\boldsymbol{\Theta}$ as,

$$\boldsymbol{\Theta} = [\boldsymbol{\theta}_1 \quad \boldsymbol{\theta}_2 \quad \dots \quad \boldsymbol{\theta}_N]_{LN_s \times N}, \quad (9)$$

then we have

$$\mathbf{r} = \boldsymbol{\Theta} \times \mathbf{z} + \mathbf{n} \quad (10)$$

where $\mathbf{r} \triangleq [r_1^T \quad r_2^T \quad \dots \quad r_L^T]^T_{LN_s \times 1}$ is the vector of all L received signals, $\mathbf{z} \triangleq [\zeta_1 \quad \zeta_2 \quad \dots \quad \zeta_N]^T_{N \times 1}$ is the sparse vector of z -values assigned to each grid point and \mathbf{n} is the noise. Now, we can solve our problem by forming the regularized *BPDN (Basis Pursuit Denoising) problem* [17] as:

$$\hat{\mathbf{z}} = \arg \min \left\| \boldsymbol{\Theta} \times \mathbf{z} - \mathbf{r} \right\|_2 + \lambda \left\| \mathbf{z} \right\|_1 \quad (11)$$

where $\|\cdot\|_p$ is the ℓ_p -norm defined as $\|v\|_p = \sqrt[p]{\sum_i |v_i|^p}$.

III. SIMULATION RESULTS

We examined the performance of the proposed method using Monte Carlo computer simulation with 500 runs each time for various numbers of sensors (4, 6, 8, 10, 12, 14 and 16 sensors) in multipath and shadowing conditions. We generated the random Gaussian variable S in equation (2) with the variance available in table (1). We assumed that the sensors are mounted on the surface of human torso equally spaced or mounted in a wearable jacket (as shown in figure 1-(b)) and the locations of the target and the reflector points have been chosen randomly. In this simulation, we used an BPSK signal with frequency of 405 MHz and bandwidth of 300 KHz which is consistent with Medical Implant Communication Services (MICS). The grid size is (1×1) cm and the randomly chosen capsule location is (10.6, 6.2) cm in the x-y plane. We ran this simulation for two SNR values (-10dB and 0dB).

Figure 2 shows the RMS Error vs. number of sensors for estimating the location of the capsule in (x,y) plane and Figure3 shows the Standard Deviation of the location estimation vs. number of sensors. As we expected, the accuracy gets better by increasing the number of the sensors. As we see, the results show that the proposed method has very good performance even for low SNRs.

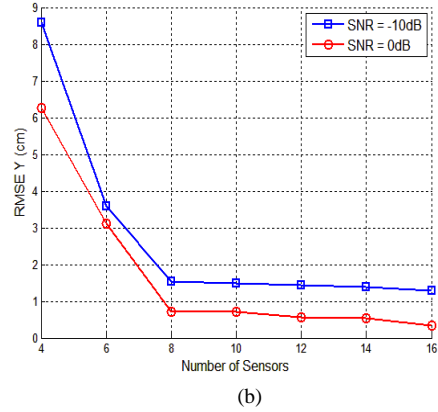
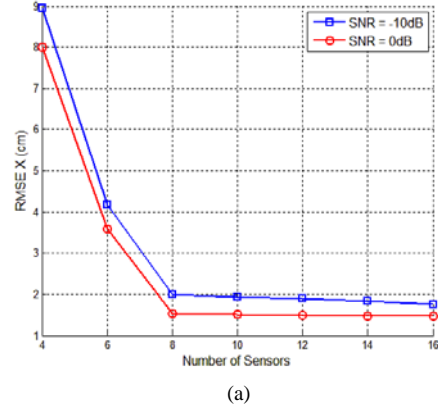


Figure (2): RMS Error for X and Y (cm) versus Number of sensors for two cases SNR = 0 dB and SNR = -10 dB.

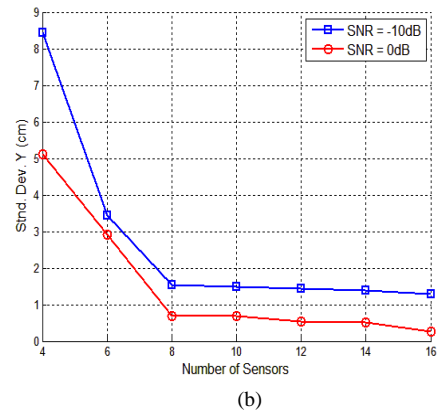
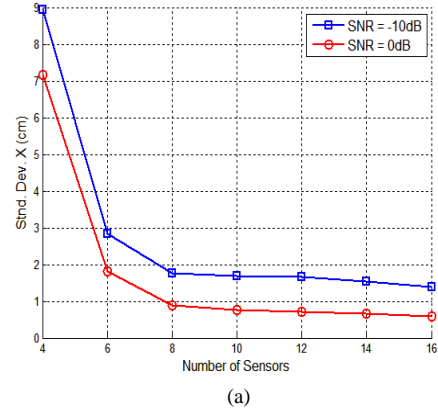


Figure (3): Std. Dev. for X and Y (cm) versus Number of sensors for two cases SNR = 0 dB and SNR = -10 dB.

IV. CONCLUSION

Recently, Wireless Capsule Endoscopy (WCE) has become the preferred method to visualize and diagnose the human gastrointestinal (GI) tract. The accurate estimation of capsule location plays a critical role in capsule endoscopy since the physicians need to know the exact location of the capsule in the endoscopy process. In this paper, we developed a method to estimate the location of the wireless capsule using both time-of-arrival (TOA) and received signal strength (RSS) based on the spatial sparsity of the emitter (capsule) in 3D space. As mentioned before, some challenges exist for in-body localization due to the complex nature within the human body, such as multipath issue caused by the boundaries of organs, shadowing effect, the dependency of the signal propagation velocity on tissue type and the dependency of the path loss parameters on the tissue thickness (deep or near surface). The restrictions on signal bandwidth and signal power also make it more challenging to achieve accurate location estimation. In our method, we directly estimate the location of the capsule (as emitter) without going through the intermediate stage of TOA or signal strength estimation. To achieve an accurate estimation, we estimate the average propagation velocity and path loss parameters for the path from each grid point to the sensors. In this method, we assign a non-zero number to each one of the grid points containing the emitter (capsule) and zero to the rest of the grid points. Thus, the vector formed from these numbers will be a sparse unknown vector that we aim to estimate. Since each element of this vector corresponds to one grid point in the grid space, we can estimate the location of the emitter by extracting the position of non-zero elements of the sparsest vector that satisfy the delay and path loss relationship between transmitted signals and received signals. We evaluated the performance of the proposed method using Monte-Carlo simulation for various numbers of sensors and various SNRs (with 500 runs each time). The simulation results show that the proposed method is very accurate in location estimation even with small number of sensors. Furthermore, the system demonstrates robust operations in noisy environments with low SNRs, which means that even with very low transmitted power (in order to reduce the risk of interfering with other users of the same band and also to keep the implant device small with long battery life), we can achieve a high localization accuracy.

REFERENCES

- [1] Y. Wang, R. Fu, Y. Ye, U. Khan, K. Pahlavan, "Performance bounds for RF positioning of Endoscopy camera capsules", *Conference on Biomedical Wireless Technologies, Networks, Sensing Systems*, 2011.
- [2] U. Khan, K. Pahlavan, S. Makarov, "Comparison of TOA and RSS based techniques for RF localization inside human tissue", *Engineering in Medicine and Biology Society (EMBC), Annual International Conference of the IEEE*, Sep. 2011 .
- [3] Y. Ye, U. Khan, N. Alsindi, R. Fu, K. Pahlavan, "On the accuracy of RF positioning in multi-Capsule endoscopy", *International IEEE Symposium on Personal Indoor and Mobile Radio Comm.*, 2011.
- [4] M. Kawasaki , R. Kohno, "A TOA Based Positioning Technique of Medical Implanted Devices," in *Third International Symposium on Medical information & communication technology*, 2009.
- [5] K. Arshak and F. Adepoju, "Adaptive linearized methods for tracking a moving telemetry capsule," *IEEE international symposium on industrial electronics (ISIE)*, June 2007.
- [6] J. Oh, S. K. Shah, X. Yuan, and S. J. Tang, "Automatic Classification of Digestive Organs in Wireless Capsule Endoscopy Videos," in *The 22nd Annual ACM Symposium on Applied Computing, SAC07*, 2007.
- [7] M. Frisch, A. Glukhovskiy, D. Levy, "Array System and Method for Locating an in Vivo Signal Source," Patent US2002/0 173 718, 2002.
- [8] M. Fischer, R. Schreiber, D. Levi, and R. Eliakim, "Capsule Endoscopy: the Localization System," *Gastrointestinal endoscopy clinics of north america*, vol. 14, pp. 25–31, 2004.
- [9] J. Bulat, et al., "Data Processing Tasks in Wireless GI Endoscopy: Image-based Capsule Localization and Navigation with Video Compression," in *Proc. of IEEE/EMBS*, 2007, pp. 2815–2818.
- [10] R. Kuth, J. Reinschke, and R. Rockelein, "Method for Determining the Position and Orientation of an Endoscopy Capsule Guided Through an Examination Object by Using a Navigating Magnetic Field Generated by Means of a Navigation Device," Patent US2007/0 038 063,
- [11] K. Sayrafian-Pour, et al., "A statistical path loss model for medical implant communication channels," in *Personal, Indoor and Mobile Radio Communications, IEEE 20th International Symposium on*, 2009.
- [12] R. G. Baraniuk. "Compressive Sensing". *IEEE Signal Processing Magazine*, 118–120, July 2007.
- [13] R. E. Blahut, "Theory of remote surveillance algorithms, The IMA Volumes in Mathematics and Its Application, Volume 32, 1991.
- [14] M. Pourhomayoun and M. L. Fowler, "Exploiting Cross Ambiguity Function Properties for Data Compression in Emitter Location Systems", *Conference on Information Sciences and Systems CISS(2011)*, Johns Hopkins University, March 23 – 25, 2011.
- [15] C. Gabriel, "Compilation of the dielectric properties of body tissues at RF and microwave frequencies," Armstrong Laboratory, Brooks Air Force Base, Tech. Rep. puAL/OE-TR-1996-0037, 1996.
- [16] C. Gabriel, S. Gabriel, and E. Corhout, "The dielectric properties of biological tissues: Literature survey," *Phys. Med. Biol.*, vol. 41, 1996.
- [17] M. F. Duarte, Y. C. Eldar, "Structured Compressed Sensing: From Theory to Applications", *IEEE Transactions on Signal Process.*, 2011.